Low-Dimensional Representations of Inflow Turbulence and Wind Turbine Response Using Proper Orthogonal Decomposition

Korn Saranyasoontorn

Lance Manuel

Department of Civil Engineering,
University of Texas at Austin,
Austin, TX 78712

A demonstration of the use of Proper Orthogonal Decomposition (POD) is presented for the identification of energetic modes that characterize the spatial random field describing the inflow turbulence experienced by a wind turbine. POD techniques are efficient because a limited number of such modes can often describe the preferred turbulence spatial patterns and they can be empirically developed using data from spatial arrays of sensed input/excitation. In this study, for demonstration purposes, rather than use field data, POD modes are derived by employing the covariance matrix estimated from simulations of the spatial inflow turbulence field based on standard spectral models. The efficiency of the method in deriving reduced-order representations of the along-wind turbulence field is investigated by studying the rate of convergence (to total energy in the turbulence field) that results from the use of different numbers of POD modes, and by comparing the frequency content of reconstructed fields derived from the modes. The National Wind Technology Center's Advanced Research Turbine (ART) is employed in the examples presented, where both inflow turbulence and turbine response are studied with low-order representations based on a limited number of inflow POD modes. Results suggest that a small number of energetic modes can recover the low-frequency energy in the inflow turbulence field as well as in the turbine response measures studied. At higher frequencies, a larger number of modes are required to accurately describe the inflow turbulence. Blade turbine response variance and extremes, however, can be approximated by a comparably smaller number of modes due to diminished influence of higher frequencies.
[DOI: 10.1115/1.2037108]

Keywords: Proper Orthogonal Decomposition, Wind turbine, Inflow turbulence

Introduction

Proper Orthogonal Decomposition (POD) is a powerful numerical technique that is often used to extract preferred spatial "modes" or patterns of variations in a high-dimensional random field by using measured data. Mathematically, POD procedures empirically identify deterministic orthogonal basis functions (modes) that preserve the energy of fluctuations and the spatial coherence in the random field in an efficient manner. An appealing feature of the method is that it provides an optimal representation of the stochastic field compared to other linear orthogonal decomposition techniques, and is thus suited for use in deriving low-dimensional descriptions of complex random fields. By truncation of the higher modes that are associated with lower energy levels, efficient computational schemes result that can describe the random field with accuracy.

POD techniques have been widely used in many engineering applications—for example, in turbulent fluid flows [1], wind engineering [2,3], and studies related to turbulence and atmospheric stability for wind turbines [4]. The effectiveness of these techniques in describing dominant features of a high-dimensional random field as illustrated in such studies suggests possible benefits that could result from their use in characterizing the inflow turbulence field experienced by wind turbines. Such characterizations can be useful in the analysis of wind turbine loads. Also, once the inflow turbulence modes at a site have been empirically identified using POD techniques, it is possible that only a few such modes associated with high energy might suffice for accurate description of the spatial inflow turbulence structure. Moreover, it is possible that an even smaller number of these estimated inflow POD modes may be required to derive an accurate representation of the turbine loads, due to filtering effects of the structural and aerodynamic system that can render some POD modes insignificant. Finally, POD techniques can be useful in assessing which inflow characteristics most significantly drive turbine loads by investigating the response measures and loads that result from the use of different subsets of inflow POD modes.

In this preliminary study, the effectiveness of the POD procedure in identification of key spatial patterns in the inflow turbulence is of interest for the 600 kW Advanced Research Turbine (ART) that is part of an ongoing research program at the National Wind Technology Center (NWTC). We employ simulation studies of the three-dimensional inflow turbulence field influencing the rotor. Ordinarily, all three turbulence components need to be part of the decomposition procedure that we describe. However, to illustrate application of the POD techniques to wind turbine load analysis, decomposition of the along-wind inflow turbulence component alone is considered here. As we shall demonstrate later, inclusion of the across-wind and vertical components of turbulence has insignificant influence on the turbine load statistics studied. Note that cross-coherence between any pair of orthogonal turbulence components as well as the auto-coherence at all fre-

Contributed by the Solar Energy Division of THE AMERICAN SOCIETY OF MECHANICAL ENGINEERS. Manuscript received by the ASME Solar Division March 27, 2005; final revision July 7, 2005. Associate Editor: D. Berg.

quencies and separations of the across-wind and vertical turbulence components are usually small and are assumed to be zero here. While such an assumption is not required to be made, since the POD procedure can be applied in the general case that might involve all components with nonzero coherence and cross-coherence, the most important influences are fully accounted for in the illustrations presented, and the benefits of the procedure are expected to be similar.

We begin with a brief review of the theoretical framework for POD analysis. The effectiveness of the method will be assessed by studying the energy of empirically derived orthogonal (and uncorrelated) sub-processes of a inflow field simulated based on the Kaimal spectral model and the IEC exponential coherence model, recommended in the IEC guidelines [5] for wind turbine design (see the Appendix for details about these models). The accuracy of reduced-order inflow representations using a limited number of POD modes to describe the target along-wind turbulence field is studied. The frequency content of the original turbulence field and that of its low-dimensional representation are also compared. To evaluate the efficiency of the POD procedure in characterizing wind turbine response, we employ reconstructed inflow fields based on different numbers of POD modes as input to a wind turbine response simulator. Statistics of various turbine response measures are estimated from the time series that use a reduced-order response representation and these are compared with the original (target) response time series.

Proper Orthogonal Decomposition

In the following, we present the key concepts upon which Proper Orthogonal Decomposition is based. Several references related to these techniques can be found in the literature (see, for example, Refs. [1,2]).

In one form of Proper Orthogonal Decomposition, called in some places Covariance Proper Transformation (CPT), assume that one is given N weakly stationary (second-order stationary) zero-mean correlated random processes $\boldsymbol{V}(t) = \{V_1(t), V_2(t), \ldots V_N(t)\}^T$ and a corresponding $N \times N$ covariance matrix, $\mathbf{C_V}$. It is possible to diagonalize $\mathbf{C_V}$ so as to obtain the (diagonal) matrix, $\mathbf{\Lambda}$.

$$\mathbf{\Phi}^T \cdot \mathbf{C_V} \cdot \mathbf{\Phi} = \mathbf{\Lambda}; \quad \mathbf{C_V} \cdot \mathbf{\Phi} = \mathbf{\Phi} \cdot \mathbf{\Lambda}; \quad \mathbf{\Lambda} = \mathrm{diag}\{\lambda_1, \lambda_2,, \ldots \lambda_N\} \tag{1}$$

The eigenvectors, $\mathbf{\Phi} = \{\boldsymbol{\phi}_1, \boldsymbol{\phi}_2, \ldots \boldsymbol{\phi}_N\}$ of $\mathbf{C_V}$ describe basis functions in a principal space. It is now possible to rewrite the original N correlated processes, $\boldsymbol{V}(t)$, in terms of N uncorrelated scalar processes, $\mathbf{Z}(t) = \{Z_1(t), Z_2(t), \ldots Z_N(t)\}^T$ such that

$$\boldsymbol{V}(t) = \mathbf{\Phi} \cdot \boldsymbol{Z}(t) = \sum_{j=1}^{N} \boldsymbol{\phi}_j Z_j(t) \tag{2}$$

where the uncorrelated scalar processes can be derived by employing the orthogonality property,

$$\boldsymbol{Z}(t) = \mathbf{\Phi}^T \cdot \boldsymbol{V}(t) \tag{3}$$

The covariance matrix for $\boldsymbol{Z}(t)$, namely $\mathbf{C_Z}$, is equal to the diagonal matrix, $\mathbf{\Lambda}$, and an energy measure associated with each $Z_j(t)$ can be defined in terms of its variance, λ_j. The original random processes are conveniently decomposed into N uncorrelated random processes. If the eigenvalues, $\mathbf{\Lambda}$, are sorted in decreasing order, a reduced-order representation, $\hat{\boldsymbol{V}}(t)$, is obtained by only retaining the first M covariance-based POD modes as follows:

$$\hat{\boldsymbol{V}}(t) = \sum_{j=1}^{M} \boldsymbol{\phi}_j Z_j(t), \quad \text{where } M < N \tag{4}$$

Note that in the description above, $\boldsymbol{V}(t)$, can represent scalar wind speed (turbulence) random processes at N different locations defined for a single direction (such as along-wind), but it could also represent all three components of turbulence at various locations. Clearly, an extension of the POD technique to model a three-dimensional turbulence field is straightforward, even though only along-wind turbulence is considered here.

Fig. 1 The National Wind Technology Center's Advanced Research Turbine (ART) used in the numerical studies

An attractive feature of the POD procedure is that the derived low-dimensional representation of a weakly stationary Gaussian random process is optimal compared to any other linear orthogonal decomposition [1,6,7]. In the present study, as is discussed next, CPT will be employed to decompose a simulated inflow turbulence random field.

Numerical Examples

In this section, the accuracy of reduced-order inflow turbulence representations based on covariance proper transformation (CPT) in describing the along-wind turbulence field as well as the structural response of a wind turbine is assessed. For the sake of illustration, 19 ten-minute simulations of a wind turbulence vector random field were generated with a sampling frequency of 20 Hz over the rotor plane of the National Wind Technology Center's Advanced Research Turbine (ART). This turbine, see Fig. 1, is a Westinghouse 600 kW, upwind, two-bladed teetered-hub turbine with a hub height of 36.6 m, a rotor diameter of 42 m, and a constant rotor speed of 42 rpm [8]. The computer program, SNwind [9,10], was used for carrying out the three-dimensional inflow field simulation. The Kaimal spectral model and the IEC exponential coherence model recommended in the IEC guidelines [5] for wind turbine designs were assumed for the inflow simulation.

For the inflow field simulation, a 6×6 square grid discretization of the rotor plane (with a vertical and lateral grid spacing of 8.4 m) was used as shown in Fig. 2. The node numbers are also

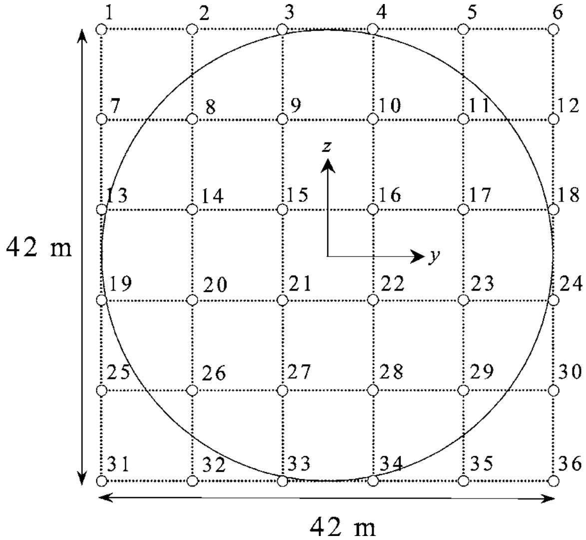

Fig. 2 Thirty-six spatial locations on the 42 m×42 m rotor plane of the ART machine used in the POD analyses

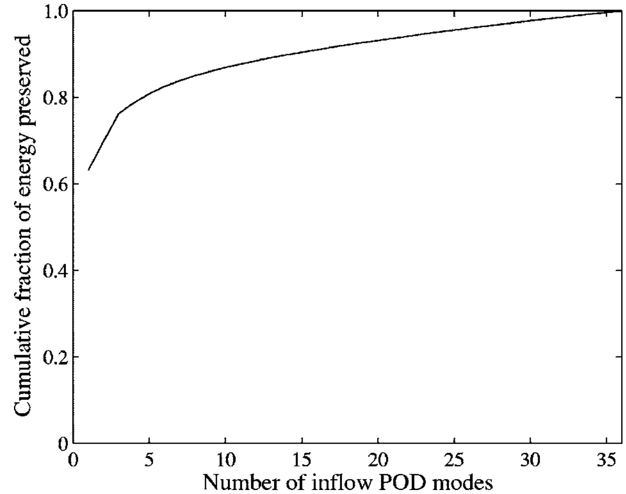

Fig. 4 Cumulative fraction of energy in low-order representations of along-wind turbulence

given in Fig. 2 for easy reference. Since only the along-wind turbulence component is considered in modeling the turbulence field, a total of 36 inflow turbulence POD modes can be defined to represent this field. In the following, we first discuss the accuracy of reduced-order representations of the simulated turbulence field.

POD Representation of the Inflow Turbulence Field. The along-wind inflow turbulence POD modes are empirically derived by employing covariance proper decomposition (CPT). A 36 ×36 covariance matrix is obtained using sample variance and covariance estimates resulting from a concatenation of all of the 19 ten-minute simulations of the spatial inflow turbulence field. The eigenvalues, λ_j, associated with the energy of each POD mode are computed and shown in Fig. 3. Clearly, the first POD mode accounts for a considerably large contribution of the total energy compared with the energy from the other modes. Further, it is seen from the plot of the cumulative fraction of energy preserved in low-order representations of the along-wind turbulence field in Fig. 4 that the first mode alone carries almost 65% of the total energy of the turbulence field while approximately 80% of the total energy is captured by the first five POD modes. It should be mentioned here that reduced-order POD representations are especially efficient when the stochastic random field under consideration is strongly correlated over different spatial scales, which is the case for the along-wind turbulence component (this is why projections of the original field onto the very first few modes preserve a large proportion of the energy in along-wind turbulence.) The other two orthogonal turbulence components typically exhibit relatively weaker correlation [11]; hence, the usefulness of the POD procedure may be limited for these other turbulence components. The first nine (out of 36) energetic eigenmodes of the simulated along-wind turbulence field are illustrated in Fig. 5. The percentage of energy (variance) corresponding to each POD mode, λ_j, of the entire turbulence field is also indicated in the figure. It is clear from the figure that the first mode, which accounts for the largest amount of energy in the turbulence field, describes a mostly uniform spatial inflow pattern over the rotor plane, while the second and third modes (each with similar energy levels) describe sheared turbulence patterns in the vertical and lateral directions, respectively. As expected, the patterns of inflow turbulence in higher modes, such as modes 4–9 shown in Fig. 5, become increasingly complex when compared with those of the first three modes [12].

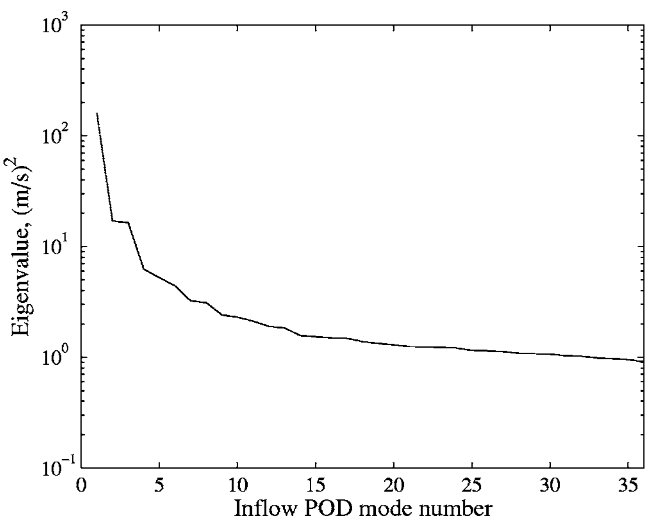

Fig. 3 Eigenvalues of the covariance matrix of the along-wind turbulence for each POD mode

Convergence to the variance in inflow turbulence at each spatial location over the rotor plane with different low-order representations (using 1 and 10 POD modes) is demonstrated in Fig. 6. It is found that the convergence rates at different locations are quite different. With the first mode alone, the variance of the along-wind turbulence at locations near the center of the rotor is closer to the target when compared with locations near the edge of the rotor plane. With an increase in the number of the POD modes included, the variance at all locations is estimated with similar levels of accuracy. This is because the eigenmodes beyond the first that describe spatial shear of the inflow turbulence and other nonuniform patterns (see Fig. 5) are needed, especially at locations away from the center. These results suggest that with the first few modes, the variance (or energy) of the reconstructed turbulence field is primarily concentrated near the rotor center; after a sufficient number of additional modes are included, the energy of the turbulence field tends to get more accurately represented at all locations on the rotor plane.

Reconstructed time series of the along-wind turbulence at node number 15 on the rotor plane (as defined in Fig. 2) based on 1, 5, and 10 inflow modes are plotted in Fig. 7, along with the target time series simulated using SNwind. Only a single 10 min segment is shown here. It is seen that when a small number of POD modes are employed, the low-frequency characteristics in the in-

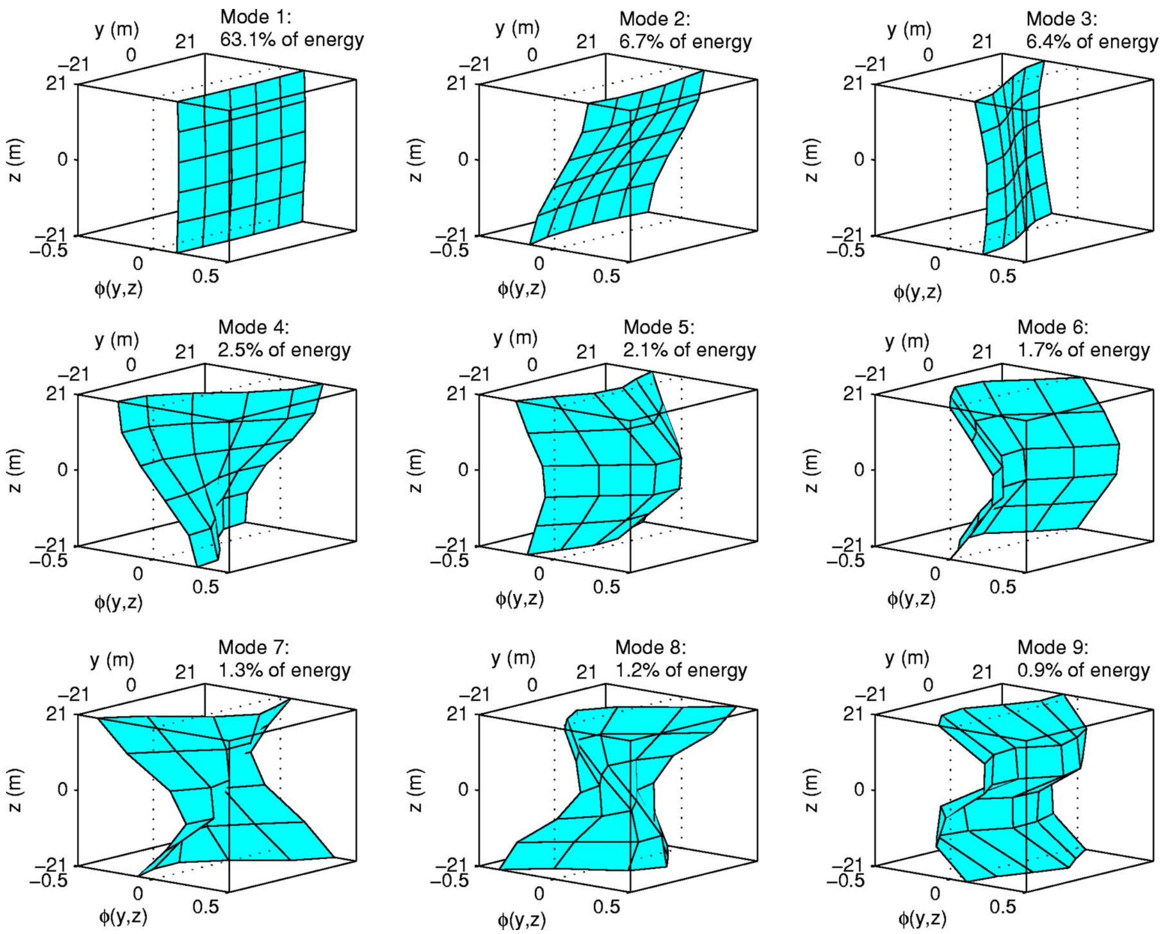

Fig. 5 First nine eigenmodes and corresponding fractions of eigenvalues of the covariance matrix of the along-wind turbulence field

flow are captured quite accurately. To obtain a good representation of the high-frequency content, however, a larger number of POD modes are required. In order to study the frequency content of the reconstructed time series in greater detail, power spectral density

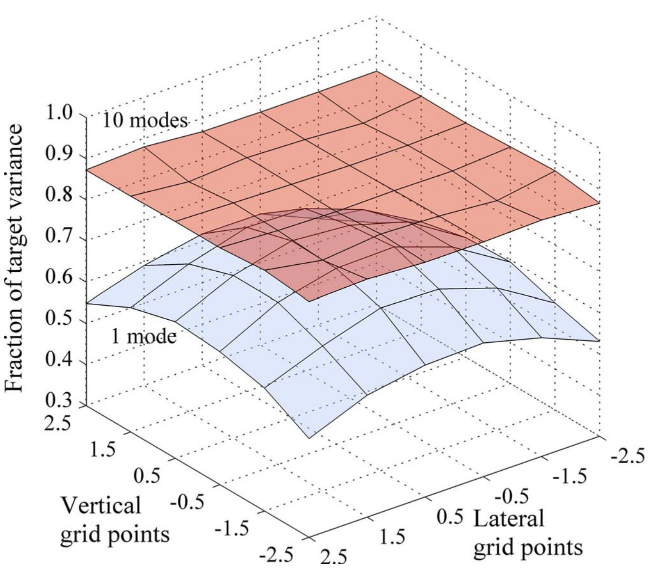

Fig. 6 Fraction of the target variance of the along-wind turbulence component at the 36 grid points on the rotor plane (see Fig. 2) based on 1 and 10 POD modes

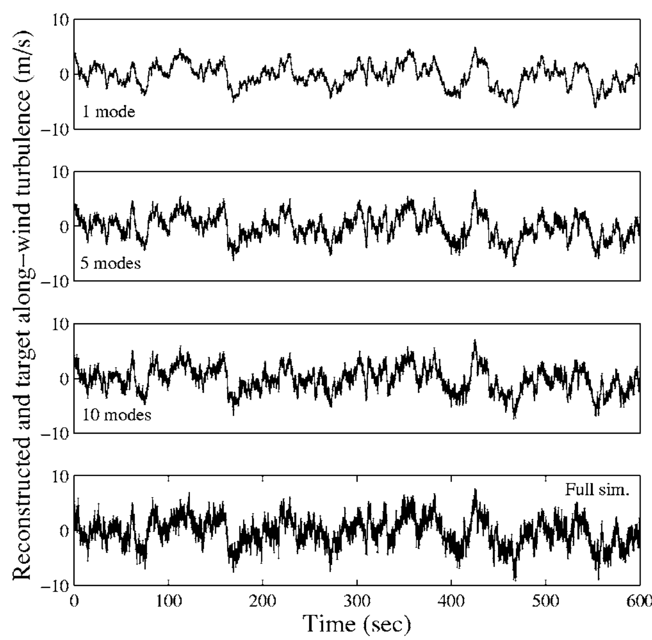

Fig. 7 Reconstructed time series of the along-wind turbulence at grid point 15 (see Fig. 2) based on 1, 5, and 10 POD modes (compared with the target)

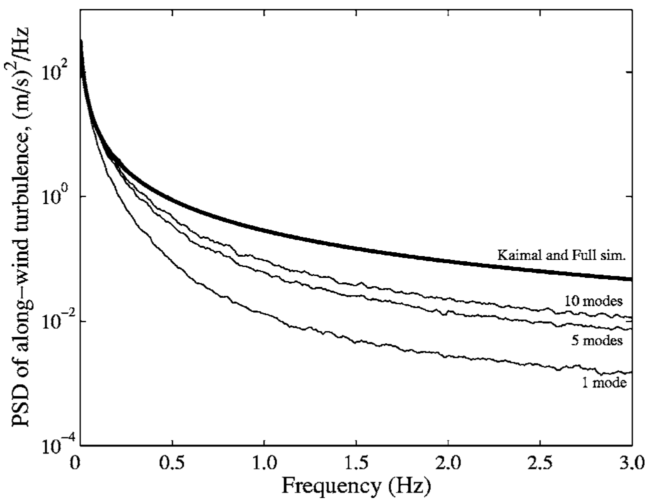

Fig. 8 PSDs of the reconstructed along-wind turbulence at grid point 15 (see Fig. 2) using 1, 5, and 10 POD modes compared with the full-field simulation and the target Kaimal spectral model

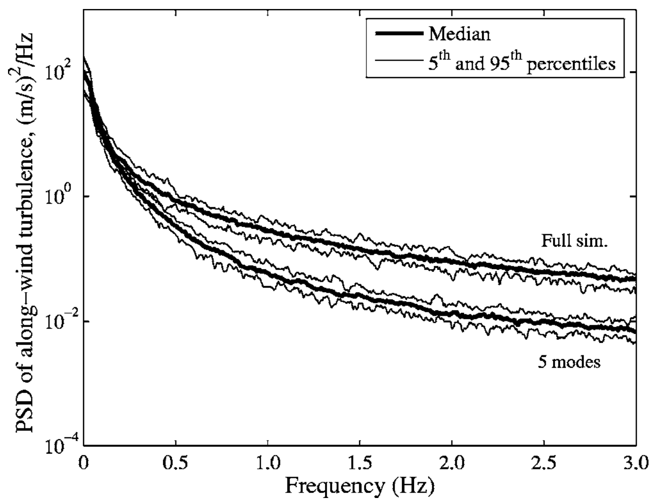

Fig. 9 Median, 5th percentile, and 95th percentile PSD estimates of along-wind turbulence at grid point 15 (see Fig. 2) using 5 POD modes compared with similar estimates from full-field simulations

functions (PSDs) from the 19 ten-minute turbulence time series at the same grid location on the rotor plane were estimated and are shown in Fig. 8. The PSDs for the reconstructed time series were estimated based upon Welch's modified periodogram method [13] using 50-percent overlapping segments, each multiplied by a Hanning data window (see, for example, [14]). The Kaimal spectral model on which the full-field simulation is based is also shown for the sake of comparison. It is seen that the PSD of the SNwind-simulated time series matches the Kaimal model very well. The plot confirms our statement that only a small number of POD modes are needed to accurately describe the low-frequency inflow energy while a much larger number may be required at higher frequencies. This is mainly because the turbulence field is more coherent at low frequencies, as has been verified in many experimental results (see, for example, Refs. [11,15]) and, hence, the efficiency of the POD procedure is more obvious in the low-frequency range.

To ensure that employing a reduced-order POD representation of the along-wind turbulence field does not introduce large variability in the inflow turbulence, the median, 5th percentile, and 95th percentile of the PSD estimates from the 19 ten-minute reconstructed inflow turbulence time series at node number 15 based on 5 POD modes, as well as similar PSD estimates based on full-field simulation, are compared in Fig. 9. It is clear from the figure that the variability in PSD estimates at all frequencies is small with the 5 POD modes and, more importantly, the relative variability is comparable with that from full-field simulations. This suggests that employing the POD procedure to describe the along-wind turbulence field does not introduce additional variability above that present in the target turbulence random field approximated by the reduced-order POD representation.

Finally, we investigate coherence in along-wind turbulence as estimated by using reduced-order POD representations. Figures 10 and 11 show coherence spectra based on reconstructed time series data from 1, 5, and 10 POD modes for two different lateral separations of 8.4 (between node numbers 15 and 16) and 25.2 meters (between node numbers 14 and 17). The target coherence spectrum based on the IEC exponential coherence model and the coherence spectrum based on full-field simulation are also included in the figures for the sake of comparison. It is seen that the coherence derived from a single POD mode is equal to unity at all frequencies, indicating perfect correlation (due to the single subprocess used for all spatial locations) as was discussed before. It is also seen that the first five POD modes are almost sufficient to describe the coherence at the larger separation of 25.2 meters. Over shorter separations, especially at higher frequencies, additional modes are necessary in order to reduce the overly large correlation that results when too few POD modes are included.

Contribution of Inflow Modes on Turbulence Response. Reconstructed along-wind turbulence time series, with several choices for the retained number of empirical orthogonal modes, are used to perform wind turbine simulations. Though the other two orthogonal turbulence components (across-wind and vertical) are not considered in the POD analysis as was discussed earlier, the turbulence fields for these two components as obtained from the SNwind simulations are added to the reduced-order along-wind turbulence while carrying out the wind turbine simulation. Our intent here is to illustrate how low-dimensional representations of the along-wind turbulence field based on the POD procedure may be applied in wind turbine load analysis. We are interested in determining how much each inflow POD mode

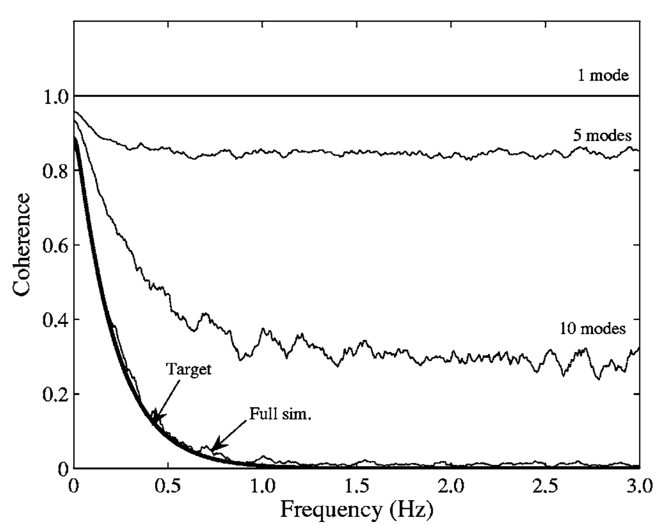

Fig. 10 Coherence spectra of the reconstructed along-wind turbulence components at a lateral separation of 8.4 m (between grid points 15 and 16) using 1, 5, and 10 POD modes compared with the full-field simulation and the target IEC exponential coherence model

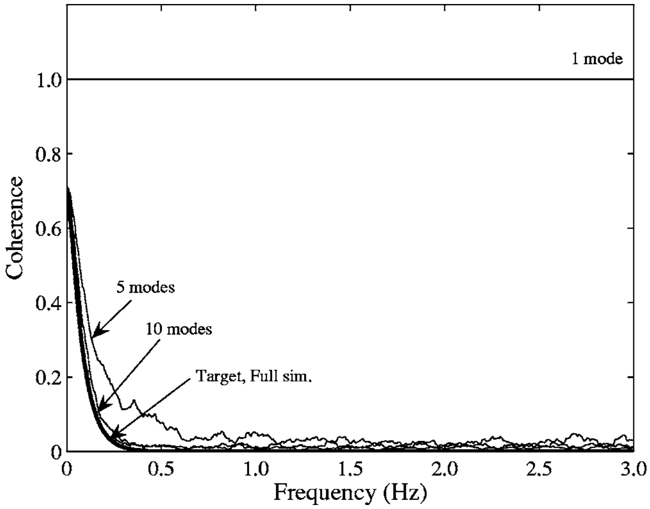

Fig. 11 Coherence spectra of the reconstructed along-wind turbulence components at a lateral separation of 25.2 m (between grid points 14 and 17) using 1, 5, and 10 POD modes compared with the full-field simulation and the target IEC exponential coherence model

contributes to various wind turbine response measures or, equivalently, how many distinct inflow field patterns are required to accurately represent the turbine response characteristics. The computer program, FAST (Fatigue, Aerodynamics, Structures, and Turbulence) [16], is employed to carry out the wind turbine simulations. The input inflow data for FAST are based on the results from POD analyses for the 19 ten-minute simulated along-wind turbulence time series (along with the across-wind and vertical turbulence time series) resulting from SNwind runs. Our main interest is in the comparison of various turbine response statistical estimates based on different numbers of POD modes; these include estimates of the variance and ten-minute extremes of (i) flapwise bending moment at the blade root, (ii) edgewise bending moment at the blade root, and (iii) fore-aft base bending moment of the tower. These turbine response statistics are studied here because they are commonly considered in wind turbine design. To achieve good estimates of turbine response statistics, a large number of ten-minute time series are generally required. However, in this preliminary study, only 19 ten-minute inflow time series are used for illustration purposes.

Figure 12 shows plots of the first 200 s of the response time series (out of a total of $19\times 600=11400$ s of available data) derived from using 1, 5, and 10 inflow POD modes as input to FAST in comparison with the target turbine response derived from the full-field inflow simulation. Zoomed-in response plots over a 10 -second duration are shown in Fig. 13 in order to emphasize the finer details in the original and the POD-based signals. As with the inflow turbulence time series, by visual inspection of Figs. 12 and 13 it can be seen that a few inflow POD modes are able to capture much of the low-frequency character of the target turbine response (at least for the blade bending response measures) but they miss the high-frequency content that might be of importance in wind turbine fatigue and extreme loads analysis. A larger number of inflow modes are required to describe the high-frequency response fluctuations. This is verified by studying the frequency content of the various response signals by means of power spectra in Figs. 14, 15, and 16, respectively, for flapwise bending moment at the blade root, edgewise bending moment at the blade root, and fore-aft tower bending moment at the base. It is clear from these figures that only a few inflow modes are needed to describe the low-frequency content in the turbine response. Peaks in the response spectra due to rotational sampling at 0.7 Hz (1P), 1.4 Hz (2P), 2.1 Hz (3P), etc. and due to the first fore-aft tower bending

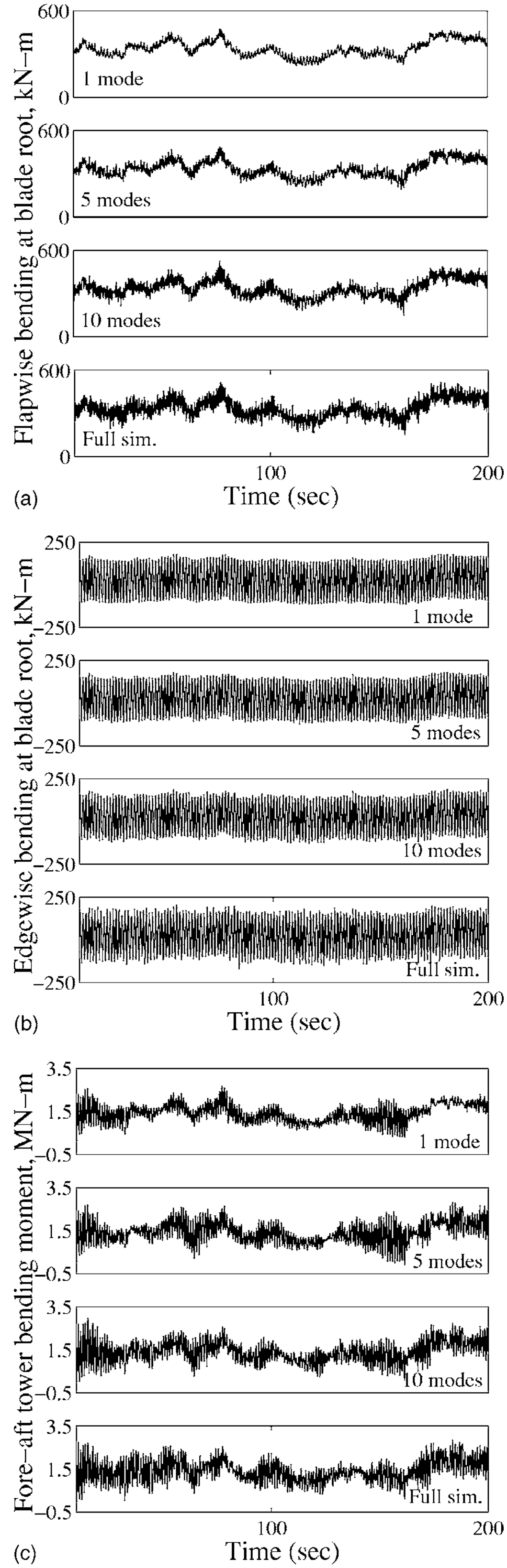

Fig. 12 Plots of (*a*) flapwise bending moment at the blade root, (*b*) edgewise bending moment at the blade root, and (*c*) fore-aft tower base bending moment derived from 1, 5, and 10 POD inflow modes compared with full-field simulations

natural frequency (around 0.85 Hz) are approximated reasonably well by the reduced-order representations of the inflow turbu-

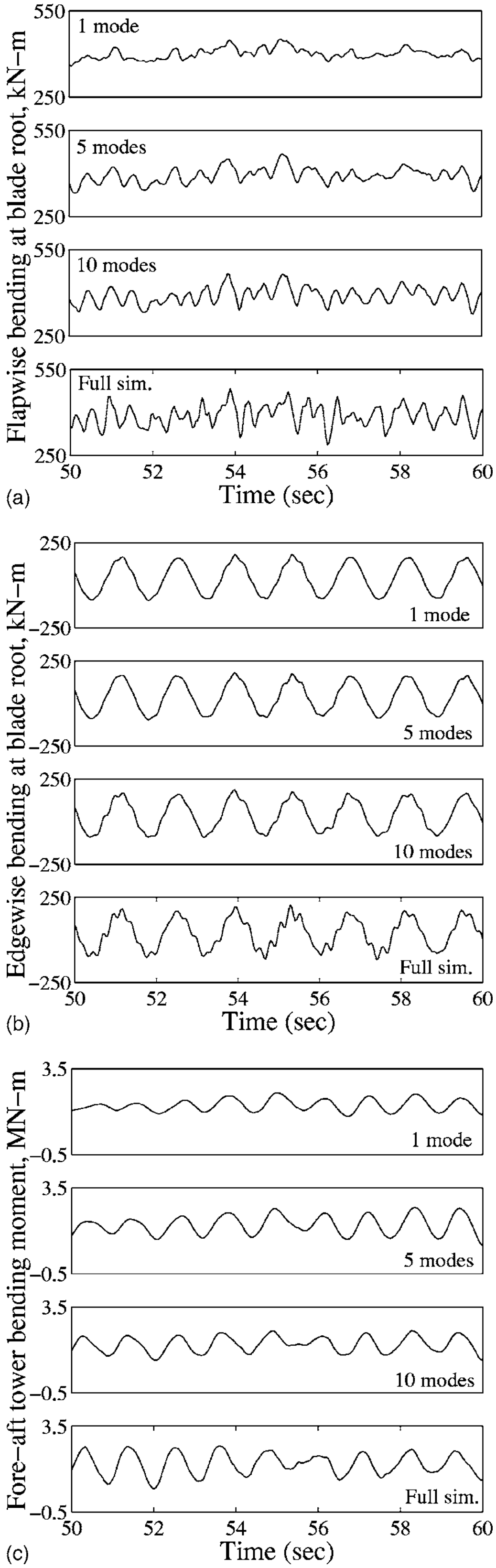

Fig. 13 Zoomed-in 10 s plots of (*a*) flapwise bending moment at the blade root, (*b*) edgewise bending moment at the blade root, and (*c*) fore-aft tower base bending moment derived from 1, 5, and 10 POD inflow modes compared with full-field simulations

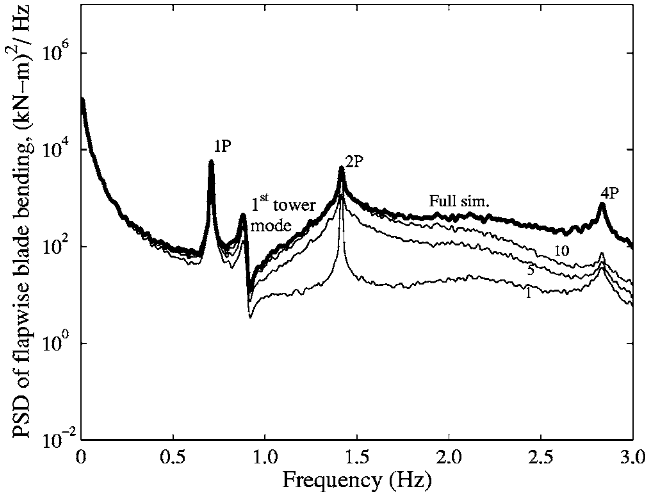

Fig. 14 Contribution of 1, 5, and 10 inflow POD modes to the PSD of the flapwise bending moment at the blade root compared with the target PSD based on full-field inflow simulations

lence. This is especially true for those peaks in the low-frequency region. A large portion of the energy (and variance) in the turbine loads studied is contributed by low frequencies; hence, only a small number of inflow POD modes may be required to derive an accurate representation of these turbine loads. For example, a single inflow POD mode appears to be adequate to represent the 1P peaks in the blade bending load spectra (see Figs. 14 and 15).

Similar to the investigation of the variability in PSD estimates of the inflow turbulence at the rotor center (Fig. 9), the median, 5th percentile, and 95th percentile PSD estimates from the 19 ten-minute flapwise blade bending moment time series based on 5 POD modes as well as on full-field inflow simulation are compared in Fig. 17. Variability in PSD estimates using 5 POD modes is seen to be small and comparable with that from full-field simulation, indicating that the POD procedure does not introduce additional variability in turbine response PSDs.

Estimates of mean values of the three turbine response measures derived using a few inflow POD modes are computed and compared with target values (from full-field inflow simulation). It is found that recovered mean values based on a single inflow POD mode closely match the target mean values in all cases. The ratio

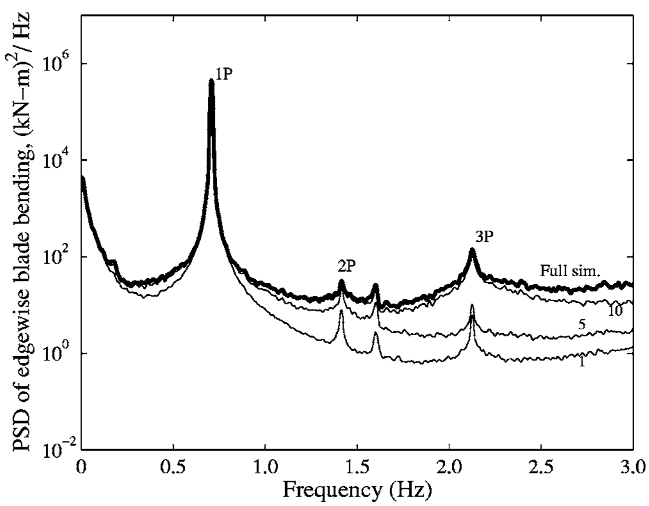

Fig. 15 Contribution of 1, 5, and 10 inflow POD modes to the PSD of the edgewise bending moment at the blade root compared with the target PSD based on full-field inflow simulations

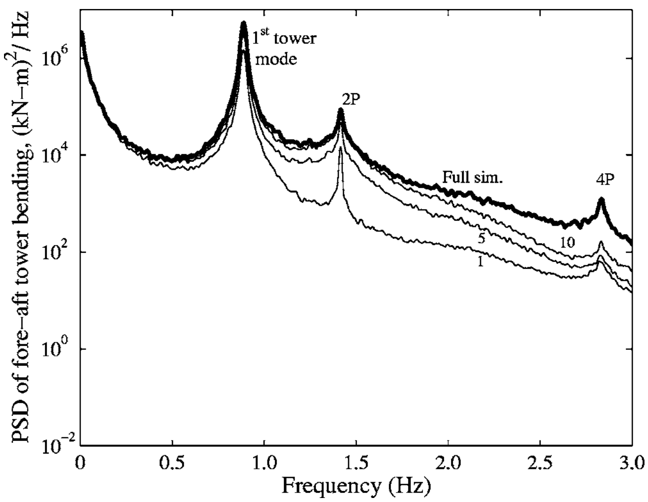

Fig. 16 Contribution of 1, 5, and 10 inflow POD modes to the PSD of the fore-aft tower bending moment at the base compared with the target PSD based on full-field inflow simulations

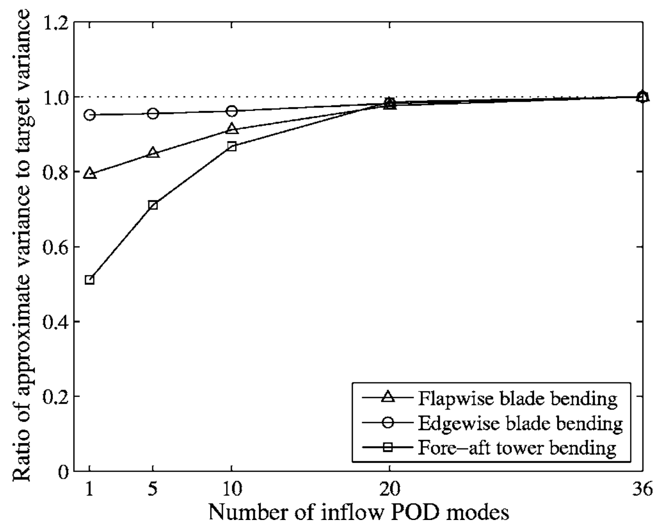

Fig. 18 Ratio of variance of turbine response measures based on 1, 5, 10, 20, and 36 POD modes to the target variance

of the approximate variance derived using 1, 5, 10, 20, and 36 inflow POD modes to the target variance for each of the turbine response measures is shown in Fig. 18. (Note that the variance is already explained in part by the PSD plots shown in Figs. 14–16.) It can be seen that only a very few inflow modes are needed to capture most of the variance in the edgewise blade bending moment loads. Physically, this is because these edgewise blade bending loads depend primarily on the rotational speed of the turbine and on gravity loading due to the self-weight of the blade, and not very much on the wind loads. The first inflow POD mode alone accounts for approximately 95% of the edgewise blade bending moment variance. For the flapwise blade bending moment and the fore-aft tower bending moment, both of which are more directly influenced by the inflow turbulence over the rotor plane, a larger number of inflow modes are needed to achieve the same accuracy that is possible with a few modes for the edgewise bending moment. Also, when comparing results for flapwise blade bending and fore-aft tower bending, it is seen that a greater number of POD modes are required for fore-aft tower bending. This is because, in the case of flapwise blade bending, comparatively more energy is concentrated at very low frequencies (see Fig. 14), where again a small number of inflow POD modes can accurately describe the inflow turbulence field. The first inflow POD mode alone accounts for approximately 80% and 50% of the variance, respectively, of the flapwise blade bending moment and the fore-aft tower bending moment processes. Overall, about five inflow POD modes may be sufficient to capture the variance (energy) in turbine blade bending loads, while for tower bending loads where the low-frequency energy is not as dominant, a somewhat larger number of inflow POD modes (say ten) may be required to achieve the same level of accuracy. Note that truncation of the higher inflow POD modes associated with small amounts of energy does not lead to as large errors in variance of blade bending loads as it does to variance in the inflow turbulence itself (Fig. 4). Again, this is due to the turbine's rotational sampling of the inflow field. Finally, Fig. 19 shows the ratio of POD-based mean ten-minute response extremes to the target mean ten-minute extreme. It is seen that with a single POD mode, turbine load extremes are within 20% of the target levels for each of the three cases. Note that the convergence rate for edgewise blade bending moment extremes is actually slower than that for the other two response measures. This is possibly due to the highly non-Gaussian char-

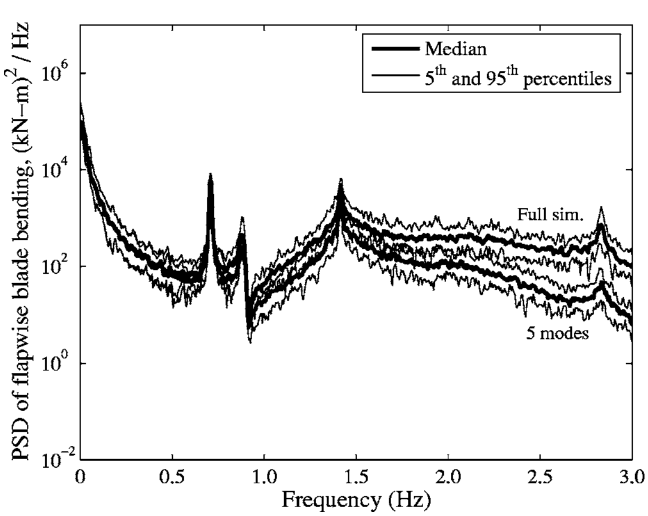

Fig. 17 Median, 5th percentile, and 95th percentile PSD estimates of flapwise bending moment at the blade root using 5 POD modes compared with full-field inflow simulations

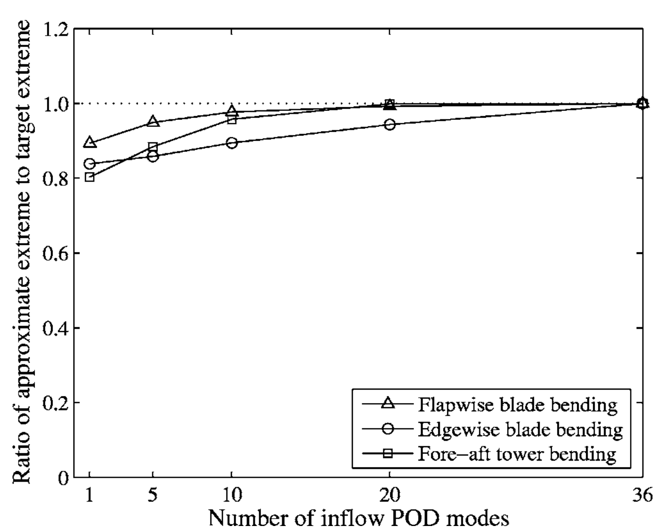

Fig. 19 Ratio of ten minute mean extreme turbine response measures based on 1, 5, 10, 20, and 36 POD modes to the target mean extreme

Table 1 Estimates of variance and mean ten-minute extreme response as a percent of corresponding estimates based on full-field simulation with inclusion of across-wind (v) and vertical (w) components in the inflow

	Variance			Mean 10 min extreme		
Turbine Response Measure	5 POD modes for u (no v and w)	5 POD modes for u (u, v, and w)	Full-field simulation (no v and w)	5 POD modes for u (no v and w)	5 POD modes for u (u, v, and w)	Full-field simulation (no v and w)
Flapwise bending	84.5	84.9	99.6	93.6	94.9	99.6
Edgewise bending	95.3	95.5	99.8	83.6	85.7	98.9
Fore-aft tower bending	68.4	70.4	98.1	87.2	88.4	99.5

acter of the edgewise blade bending process. Even though reduced-order POD representations can be accurate for edgewise bending loads variance, the convergence with number of inflow modes of higher moments (such as skewness and kurtosis) important for predicting extremes should be studied.

Discussion on the Effect of Across-Wind and Vertical Turbulence Components on Turbine Response. In this study, the empirical orthogonal decomposition of the inflow turbulence random field has been carried out only for the along-wind (u) turbulence field. The across-wind (v) and vertical (w) components have not been involved in the POD analysis only because the IEC exponential coherence model used here does not specify correlation in v (or w) turbulence signals at different spatial locations nor any cross-coherence between pairs of orthogonal turbulence components. This implies that the assumed v and w turbulence fields are already in their principal components and hence there is no reason to apply the POD procedure to search for new principal bases for these two components. Another reason for not using the POD procedure with the v and w turbulence field is that these components sometimes play an insignificant role, compared to the along-wind (u) turbulence component, in establishing turbine design loads. For instance, for the three turbine response measures studied here, very small reduction in load statistics such as variance and extremes are seen to result when the v and w inflow turbulence components are completely ignored, as seen in Table 1. For all turbine response measures, and whether one considers the full-field simulation case or the use of 5 POD inflow modes for the u component, errors in response variance and ten-minute mean extreme from ignoring v and w turbulence are less than 3%. It is important to remember, though, that these results are based on the assumption that there is no correlation of v- and w-turbulence components at different spatial locations and that there is also no correlation among the three turbulence components. Any introduction of cross-coherence among the three turbulence components (e.g., between the u- and w- components) might possibly lead to some influence of turbulence components other than the along-wind component alone. The POD procedure can easily be extended to establish full three-dimensional inflow turbulence field representations in such cases.

Conclusions

In this study, Proper Orthogonal Decomposition (POD) techniques have been employed to characterize a simulated along-wind turbulence field assumed to be experienced by a wind turbine. Different numbers of inflow POD modes have been considered in low-dimensional representations of the turbulence field. It has been found that a significant portion of the energy in the along-wind turbulence came from the first few POD modes. Using a small number of POD modes, the low-frequency characteristics of the simulated turbulence field can be approximated reasonably well. To achieve a good representation of the high-frequency content in the inflow turbulence, however, a larger number of POD modes are required. The contribution of different numbers of inflow POD modes of the along-wind turbulence to turbine structural response has also been studied. Reconstructed wind turbulence time series over 36 grid points on the rotor plane, with several choices of number of empirical orthogonal modes, have been used to perform wind turbine response simulations on the National Wind Technology Center's Advanced Research Turbine (ART) in order to illustrate how well low-dimensional representations of the inflow turbulence field can describe wind turbine loads/responses. Across-wind and vertical turbulence components have been included in the inflow simulations but no POD analyses have been required for these turbulence components based on the assumed coherence models. Results suggest that the low-frequency energy in each turbine response measure is represented reasonably well by the inclusion of only a small number of inflow POD modes. Truncation of the higher inflow POD modes associated with small amounts of energy does not reduce the turbine response variance significantly as long as the energy of the turbine response measure under consideration is mostly concentrated in the low-frequency region, where a small number of inflow POD modes can accurately describe the inflow turbulence field. It has also been found that, with only a few inflow POD modes, turbine response extremes are close to levels based on full-field inflow simulation.

Acknowledgments

The authors gratefully acknowledge the financial support provided by CAREER Award No. 0449128 from the National Science Foundation and by Grant No. 30914 from Sandia National Laboratories. They also acknowledge help received from Dr. Alan Wright and Dr. Maureen Hand of the National Renewable Energy Laboratory (NREL) with the wind turbine simulation models.

Appendix: Spectral Models for Turbulence

Kaimal Spectral Model (Based on IEC Guidelines [5]).

$$\frac{fS_1(f)}{\sigma_1^2} = \frac{4fL_1/V_{\text{hub}}}{(1+6fL_1/V_{\text{hub}})^{5/3}} \tag{A1}$$

where V_{hub} is the wind speed at hub-height averaged over 10 min;

f is the frequency in Hertz;

S_1 is the one-sided velocity component power spectrum;

σ_1 is the velocity component standard deviation;

L_1 is the velocity component integral scale parameter.

IEC Exponential Coherence Model [5].

$$\text{coh}(r,f) = \exp(-8.8((fr/V_{\text{hub}})^2 + (0.12r/L_c)^2)^{1/2}) \tag{A2}$$

where $\text{coh}(r,f)$ is the coherency function (for the longitudinal velocity component) defined as the complex magnitude cross-spectral density at two spatial locations divided by the autospectrum function;

f is the frequency in Hertz;

r is the magnitude of the projection of the separation vector between the two points under consideration onto a plane normal to the average wind direction;

L_c is the coherency scale parameter.

For turbulence characteristics of type A as defined in the IEC guidelines [5] and for a hub-height horizontal mean wind speed of 15 m/s, the along-wind velocity component standard deviation σ_1 is 2.7 m/s. For a wind turbine with hub height greater than 30 meters, the turbulence scale parameter Λ_1 is 21.0 meters. The coherency scale parameter L_c and the integral scale parameter for the along-wind turbulence component L_1 are recommended in the IEC guidelines [5] to be $3.5\Lambda_1$ and $8.1\Lambda_1$, corresponding to 73.5 and 170.1 meters, respectively.

References

[1] Holmes, P., Lumley, J. L., and Berkooz, G., 1996, *Turbulence, Coherent Structures, Dynamical Systems and Symmetry*, Cambridge Monogr. Mech., Cambridge University Press.

[2] Li, Y., and Kareem, A., 1995, "Stochastic Decomposition and Application to Probabilistic Dynamics," J. Eng. Mech., **121**, No. 1, pp. 162–174.

[3] Carassale, L., and Solari, G., 2000, "Proper Orthogonal Decomposition of Multi-Variate Loading Processes," *Proc. 8th ASCE Joint Specialty Conference on Probabilistic Mechanics and Structural Reliability*, Notre Dame, Indiana.

[4] Spitler, J. E., Morton, S. A., Naughton, J. W., and Lindberg, W. R., 2004, "Initial Studies of Low-Order Turbulence Modeling of the Wind Turbine Inflow Environment," *Proc. of the ASME Wind Energy Symposium*, AIAA, Reno, Nevada, pp. 442–451.

[5] IEC, 1998, "Wind Turbine Generator Systems Part 1: Safety Requirements," International Electrotechnical Commission (IEC), IEC/TC 88 61400–1, 2nd ed., Geneva.

[6] Lumley, J. L., 1970, *Stochastic Tools in Turbulence*, Academic Press, New York.

[7] Chen, X., and Kareem, A., 2003, "POD in Reduced Order Modeling of Dynamic Load Effects," *Proc. 9th International Conference on Applications of Statistics and Probability in Civil Engineering (ICASP9)*, Vol. 2, San Francisco, California, pp. 1591–1598.

[8] Snow, A. L., Heberling, C. F. II, and Van Bibber, L. E., 1989, "The Dynamic Response of a Westinghouse 600 kW Wind Turbine," Rept. SERI/STR-217–3405, Solar Research Institute.

[9] Veers, P. S., 1988, "Three-dimensional Wind Simulation," Sandia National Laboratory, Rept. SAND 88–0512, Albuquerque, New Mexico.

[10] Buhl, M. L. Jr., 2003, "SNwind User' Guide," National Renewable Energy Laboratory, Golden, Colorado.

[11] Saranyasoontorn, K., Manuel, L., and Veers, P. S., 2004, "A Comparison of Standard Coherence Models for Inflow Turbulence with Estimates from Field Measurements," J. Sol. Energy Eng., **126**, No. 4, pp. 1069–1082.

[12] Saranyasoontorn, K., and Manuel, L., 2004, "On Estimation of Empirical Orthogonal Modes in Inflow Turbulence for Wind Turbines," *Proc. 9th ASCE Joint Specialty Conference on Probabilistic Mechanics and Structural Reliability*, Albuquerque, New Mexico.

[13] Welch, P. D., 1967, "The Use of Fast Fourier Transform for the Estimation of Power Spectra: A Method Based on Time Averaging Over Short, Modified Periodograms," IEEE Trans. Audio Electroacoust., **AU–15**, pp. 70–73.

[14] Oppenheim, A. V., and Schafer, R. W., 1989, *Discrete-Time Signal Processing*, Prentice-Hall.

[15] Davenport, A. G., 1961, "The Spectrum of Horizontal Gustiness near the Ground in High Winds," Q. J. R. Meteorol. Soc., **87**, pp. 194–211.

[16] Jonkman, J. M., and Buhl, M. L. Jr., 2004, "FAST User's Guide," National Renewable Energy Laboratory, Rept. NREL/EL-500–29798, Golden, Colorado.